



# Data Analysis Techniques for a Lunar Surface Navigation System Testbed

*David Chelmins, O. Scott Sands, and Aaron Swank  
Glenn Research Center, Cleveland, Ohio*

## NASA STI Program . . . in Profile

Since its founding, NASA has been dedicated to the advancement of aeronautics and space science. The NASA Scientific and Technical Information (STI) program plays a key part in helping NASA maintain this important role.

The NASA STI Program operates under the auspices of the Agency Chief Information Officer. It collects, organizes, provides for archiving, and disseminates NASA's STI. The NASA STI program provides access to the NASA Aeronautics and Space Database and its public interface, the NASA Technical Reports Server, thus providing one of the largest collections of aeronautical and space science STI in the world. Results are published in both non-NASA channels and by NASA in the NASA STI Report Series, which includes the following report types:

- **TECHNICAL PUBLICATION.** Reports of completed research or a major significant phase of research that present the results of NASA programs and include extensive data or theoretical analysis. Includes compilations of significant scientific and technical data and information deemed to be of continuing reference value. NASA counterpart of peer-reviewed formal professional papers but has less stringent limitations on manuscript length and extent of graphic presentations.
- **TECHNICAL MEMORANDUM.** Scientific and technical findings that are preliminary or of specialized interest, e.g., quick release reports, working papers, and bibliographies that contain minimal annotation. Does not contain extensive analysis.
- **CONTRACTOR REPORT.** Scientific and technical findings by NASA-sponsored contractors and grantees.

- **CONFERENCE PUBLICATION.** Collected papers from scientific and technical conferences, symposia, seminars, or other meetings sponsored or cosponsored by NASA.
- **SPECIAL PUBLICATION.** Scientific, technical, or historical information from NASA programs, projects, and missions, often concerned with subjects having substantial public interest.
- **TECHNICAL TRANSLATION.** English-language translations of foreign scientific and technical material pertinent to NASA's mission.

Specialized services also include creating custom thesauri, building customized databases, organizing and publishing research results.

For more information about the NASA STI program, see the following:

- Access the NASA STI program home page at <http://www.sti.nasa.gov>
- E-mail your question via the Internet to [help@sti.nasa.gov](mailto:help@sti.nasa.gov)
- Fax your question to the NASA STI Help Desk at 443-757-5803
- Telephone the NASA STI Help Desk at 443-757-5802
- Write to:  
NASA Center for AeroSpace Information (CASI)  
7115 Standard Drive  
Hanover, MD 21076-1320



# Data Analysis Techniques for a Lunar Surface Navigation System Testbed

*David Chelmins, O. Scott Sands, and Aaron Swank  
Glenn Research Center, Cleveland, Ohio*

National Aeronautics and  
Space Administration

Glenn Research Center  
Cleveland, Ohio 44135

Trade names and trademarks are used in this report for identification only. Their usage does not constitute an official endorsement, either expressed or implied, by the National Aeronautics and Space Administration.

*Level of Review:* This material has been technically reviewed by technical management.

Available from

NASA Center for Aerospace Information  
7115 Standard Drive  
Hanover, MD 21076-1320

National Technical Information Service  
5301 Shawnee Road  
Alexandria, VA 22312

Available electronically at <http://www.sti.nasa.gov>

# **Data Analysis Techniques for a Lunar Surface Navigation System Testbed**

David Chelmins, O. Scott Sands, and Aaron Swank  
National Aeronautics and Space Administration  
Glenn Research Center  
Cleveland, Ohio 44135

## **Abstract**

NASA is interested in finding new methods of surface navigation to allow astronauts to navigate on the lunar surface. In support of the Vision for Space Exploration, the NASA Glenn Research Center developed the Lunar Extra-Vehicular Activity Crewmember Location Determination System and performed testing at the Desert Research and Technology Studies event in 2009. A significant amount of sensor data was recorded during nine tests performed with six test subjects. This paper provides the procedure, formulas, and techniques for data analysis, as well as commentary on applications.

## **1.0 Introduction**

The National Aeronautics and Space Administration (NASA) Vision for Space Exploration, announced by President George W. Bush in 2004, calls for the safe return of astronauts to the Moon. In support of the Vision, NASA is considering methods of surface navigation for crewmembers performing extra-vehicular activity (EVA).

The Digital Communications and Navigation Branch at the NASA Glenn Research Center (GRC) has developed a mobile navigation testbed, the Lunar Extra-Vehicular Activity Crewmember Location Determination System (LECLDS), to evaluate techniques for human exploration. LECLDS consists of a Global Positioning System (GPS) receiver, an inertial measurement unit (IMU), a digital compass, a navigation processor, and a handheld display unit. LECLDS was demonstrated at the 2009 NASA Desert Research and Technology Studies (D-RATS) event held at the Black Point Lava Flow near Flagstaff, Arizona.

During the D-RATS demonstration, test subjects used the navigation testbed to walk between pre-determined waypoints. Data was collected to gauge the test subject's ability to navigate (Measures of Effectiveness, MoEs) as a function of a level of performance (Measures of Performance, MoPs) of the LECLDS testbed. Navigation data was displayed in real-time to the test subject, and raw measurements were recorded simultaneously for post-processing.

This report covers the steps taken to analyze data from D-RATS 2009. This includes a brief overview of the log formats and time alignment strategy used for LECLDS, as well as the manual techniques needed to reduce the data set to useful segments. A number of data analysis metrics are presented, with commentary on applications. Finally, recommendations are made for ways to improve the collected data to make the analysis more reliable.

## **2.0 LECLDS 2009 Logs and Data Formats**

### **2.1 Time Alignment**

LECLDS stored data in a number of different ASCII formats, with several time alignment strategies. Log files were recorded for the ground truth digital compass, the GPS interface program, the GPS information from the MATLAB navigation filter, the IMU information from the navigation filter, and the navigation filter position determination information. These logs are summarized in Table I.

TABLE I.—LECLDS DATA LOGS

Type of data	Example filename	Data delimiter	Time alignment
Digital Compass	COMPASSLOG_090109_0453.csv	Comma	System timestamp (ns)
GPS Interface	gps.log.txt	Tab	GPS time (ms) System timestamp (sec) Processor ticks (ticks/sec)
Filter GPS Log	GPSLOG_090409_0551.csv	Comma	GPS time (sec) System timestamp (ns)
Filter IMU Log	IMULOG_090409_0551.csv	Comma	System timestamp (ns)
Filter Log	NAVLOG_090409_0551.csv	Comma	GPS time (sec) System timestamp (ns)

During post-processing, time alignment between the data logs was conducted in a Microsoft Excel spreadsheet for each test run. The navigation filter GPS log was used as the authoritative source of time alignment, since it linked GPS time with the system timestamp. Next, the Filter IMU Log was imported as new columns in the same file. The difference between the IMU system timestamp and the GPS system timestamp was computed, and the IMU log file information was adjusted up and down the spreadsheet rows until the time error between the two was close to zero. In general, once the start of the two logs was synchronized, the time error between them did not grow. In the event that one of the logs skipped time (for example, the IMU recorded a double value), adjustments were made to correct the skip by deleting or adding a blank line.

After synchronizing the filter GPS log and IMU log, the navigation filter log was loaded into the same spreadsheet in a similar fashion. The filter log was then synchronized to the filter GPS log by comparing the GPS times. There was very little deviation between these logs since they both are derived from the same source of data; in most cases, no adjustment had to be made.

The GPS interface log was not synchronized with the other logs, since the Filter GPS Log already contained a subset of the data from the interface log. However, in the case of extreme data corruption, the GPS interface log was manipulated into the Filter GPS Log format and used in place of the Filter GPS Log. This is acceptable because the subset of data in question was equivalent between both logs.

## 2.2 Multiple Log Files

Frequently a single test would have many different log files associated with it. Every time the navigation processor was stopped, the Digital Compass, Filter GPS, Filter IMU, and Filter logs were re-created using a new filename, and the GPS interface log was appended. If this occurred during a test, it meant that the test data was spread across many instances of the same log. In most cases, the additional logs were appended as rows to the existing spreadsheet. There usually would be a large jump in time at the point where the log was appended; this was documented but permitted, since it was more important to have synchronization across all of the logs in Table 1.

## 2.3 Visualizing the Logs

Using the new, composite spreadsheet containing time-synchronized data, it was possible to generate KML files that allowed the walkback tests to be visualized in Google Earth. In order to make the conversion, formulas were used to convert the Cartesian position fixes for GPS and the filter into longitude, latitude, and elevation.

The latitude, longitude, and elevation formulas follow the World Geodetic System 84 (WGS84) model for Cartesian coordinates  $x$ ,  $y$ , and  $z$ . Constants  $a$  and  $g$  are defined for Earth, yielding the model:

$$a := 6378137$$

$$g := 0.081819190842622$$

$$\text{Latitude} := \tan^{-1} \left( \frac{\left( \sqrt{x^2 + y^2} - g^2 a \left( \cos \left( \tan^{-1} \frac{a \sqrt{1 - g^2} \sqrt{x^2 + y^2}}{az} \right) \right)^3 \right)}{z + \frac{g^2 a}{\sqrt{1 - g^2}} \left( \sin \left( \tan^{-1} \frac{a \sqrt{1 - g^2} \sqrt{x^2 + y^2}}{az} \right) \right)^3} \right)$$

$$\text{Longitude} := \tan^{-1} \left( \frac{x}{y} \right)$$

$$\text{Elevation} := \frac{\sqrt{x^2 + y^2}}{\cos(\text{Latitude})} - \frac{b}{\sqrt{1 - g^2} \sin(\text{Latitude})}$$

Google Earth KML files can record data as individual points or “linestrings”, which consist of a line that is drawn to connect all of the points. The linestring form of the KML file is more useful for visualizing the ground truth position fixes, since the ground truth does not have large jumps. The navigation filter position fixes are better visualized using individual points.

Additional comma-separated value (CSV) files were created from field notes to represent the recorded positions of the waypoints, antenna tower, and base camp. The positions were determined using a handheld GPS receiver, converted to KML, and loaded into Google Earth using distinctive icons.

### 3.0 Data Modifications Prior to Analysis

#### 3.1 Determining Starting and Ending Locations

The testbed began recording position fixes as soon as it was activated, and it continued to log data until it was stopped. This made analysis difficult because there was an unknown amount of time at the beginning and end of each test that did not contain useful data. These amounts of time were removed by examining the ground truth position fix points in Google Earth.

The starting point in Figure 1, for example, must be determined visually. The walkback test in this case started somewhere within the large cluster of points on the left, and proceeded to the right. The actual starting time is determined visually as the first point outside of the cluster that is in sequence with the trail to the right. In this case, the point 409831 would be chosen as the starting point for the test. The label 409831 is the GPS time of week, so this value also represents the starting time.

A similar point selection method was applied to determine the finishing time and location. The finishing location is the last point in the sequence that is still outside of the cluster of points near the end of the walk.

Once the starting and finishing times were determined, all points outside of these times were saved in a separate, isolated part of the composite spreadsheet. Only times between the start and finish were considered for data analysis.

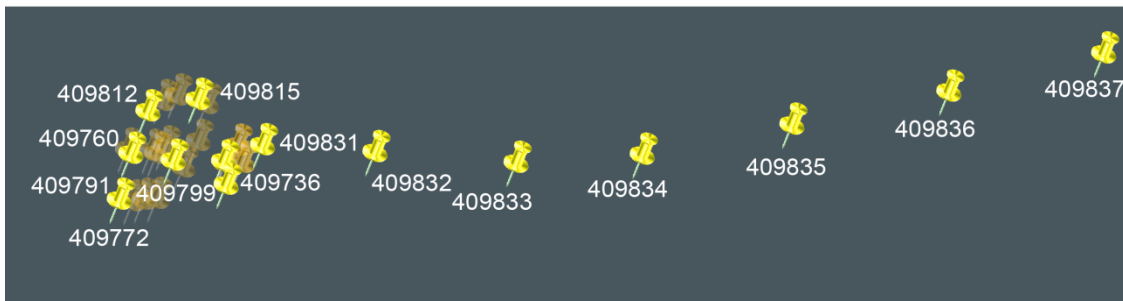


Figure 1.—Starting point surrounded by a cluster of position fixes

### 3.2 Determining Waypoint Arrival and Departure Times

In order to generate a useful data set, it was necessary to consider the individual walk segments between two waypoints. At first the entire test was analyzed as a single walk, however this was not accurate because the errors experienced by the walkback team were not uniform across the test. Based on the geometry of the radiometric nodes, certain waypoint intervals experienced larger position errors than other intervals. Averaging over the entire run did not capture the location-dependent effect of these errors.

The arrival and departure times for individual waypoints were determined visually, similar to the beginning and ending times, although with less precision. For example, the waypoint in Figure 2 has a significant amount of ambiguity. The arrival time was determined to be 410445, and the departure time could be chosen as 410528.

The difficulty in choosing arrival and departure times visually is that the choice tends to make the navigation system appear to perform better. It is possible that the team started walking at 410471 and was not sure which way to go, resulting in the clusters around 410491 and 410510. It is also possible that the team decided to take a break and just walked around the area for a minute, in which case the choice of starting location would be correct.

Another issue is that the waypoint location is subject to interpretation. In Figure 2, none of the ground truth points reached the manually-determined waypoint. Future tests must have better accuracy on the waypoint locations, or have more explicit ways of determining arrival and departure times and locations.

### 3.3 Determining Break Times

The walkback team was instructed to take periodic breaks, which were occasionally not recorded in the test log when the team did not communicate that they were planning to take a break. This presents an analysis difficulty because it was hard to determine whether the team was standing still and trying to figure out what direction to walk, or whether they were standing still while taking a break.

Many breaks were taken at waypoints, so the procedure for determining waypoint arrival and departure often took precedent. For breaks not taken at waypoints, the analysis procedure relied entirely on the hand-recorded test director's log for guidance. Even if there was a cluster of points that could be a break, this data was not removed unless the test log indicated the team took a break. This distinction is important because it preserves the "human factors" components (confusion and abrupt direction changes) of the test, as seen in Figure 3.

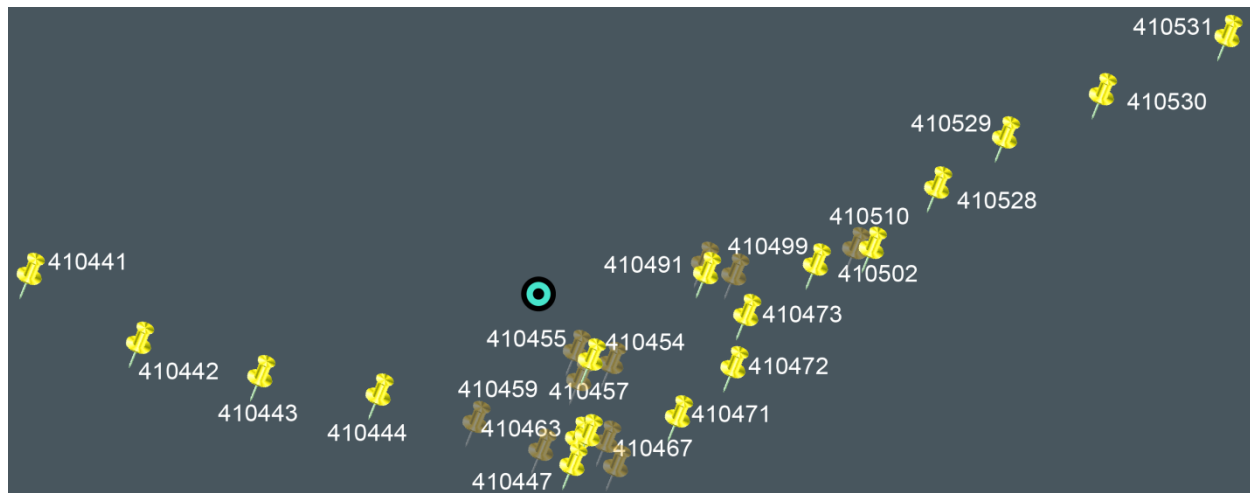


Figure 2.—Waypoint arrival and departure ambiguity



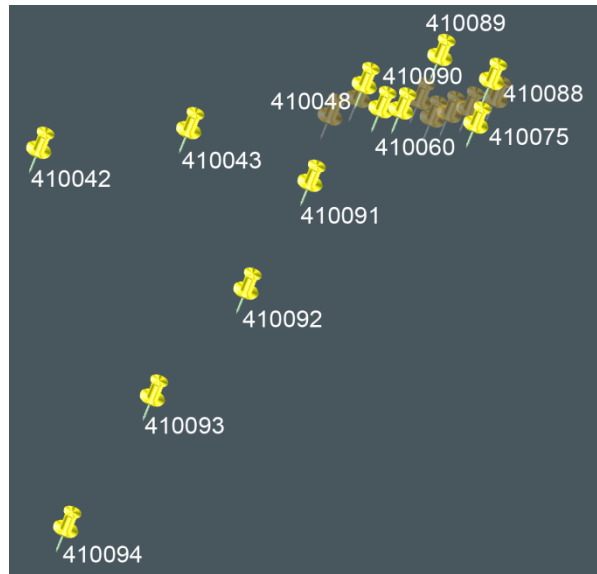


Figure 3.—Visual inspection ambiguity in determining breaks

The times between the handwritten test log and the GPS clock tend to vary from 1 to 3 min across the tests, so there is additional ambiguity when designating a portion of the data a “break”. In general, when the test log indicates the team took a break, the data is scanned for a large cluster of points around the time recorded in the test log. When these points are found, the arrival and departure time is determined and the points between the two times are removed from the analysis data set.

### 3.4 Determining System Errors and Data Corruption

Every so often the system needed to be rebooted or the software needed to be restarted to correct errors. When this occurred, multiple logs were created for the same test. System errors also affected the test subject’s interpretation of the data. Sometimes the position display did not update, and the compass remained fixed on the same heading when a system error occurred. It was not immediately clear to that the system had stopped, so the test subject continued walking on the same heading.

System errors were easy to detect in the data set because they were seen as large jumps in time or position. However, they presented an interesting problem from an analysis perspective. In general, the walkback team was walking from point A to C. The system error occurred at point B1, somewhere between A and C. The walkback team discovered the system error at point B2, which was after B1 but before arriving at C. The gap between B1 and B2 is shown in Figure 4.

When a system error occurred, the walk between two waypoints was split into two segments. The first segment covered the distance from A to B1. This segment was discarded because the team did not reach the intended waypoint C, so it was impossible to draw conclusions about how effectively they navigated to point B1 when their target was point C. The second segment, B2 to C, was analyzed by considering B2 as the starting location and C as the destination. The effectiveness of the system was then considered only over the interval B2 to C.

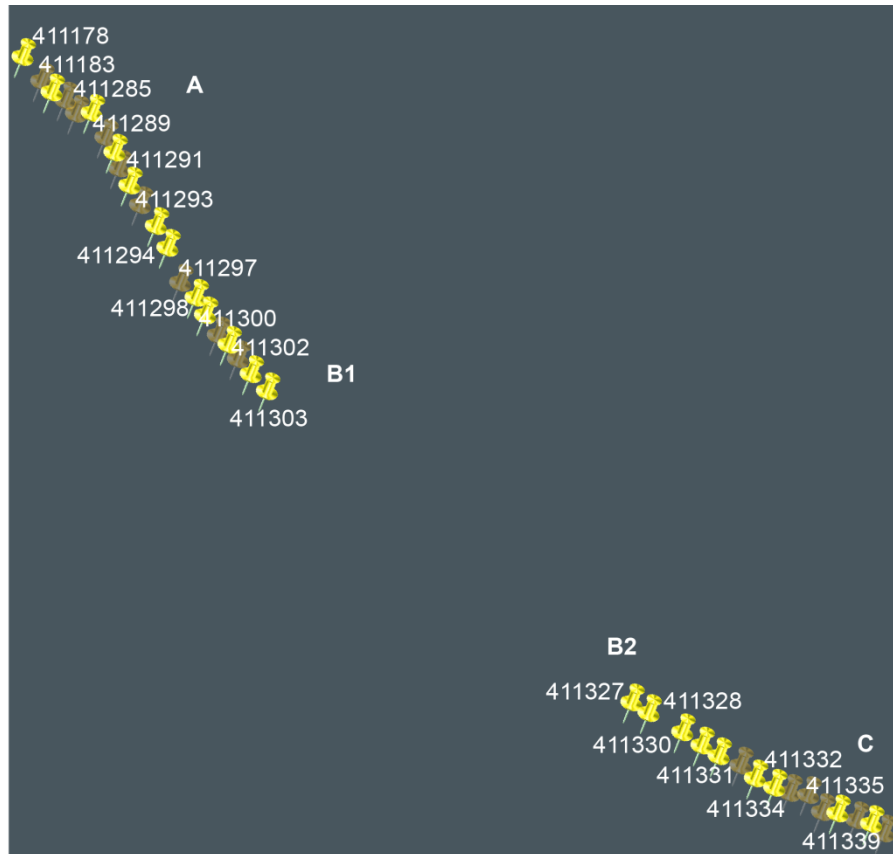


Figure 4.—Typical gap associated with a system error

### 3.5 Reconstructing the Dataset by Segments

After the entire walk was split into waypoints, breaks, and system errors, it was possible to reconstruct the dataset into individual segments. A single segment is the time and location of departure from the starting waypoint to arrival at the destination waypoint, excluding any breaks or errors between the two waypoints. The composite data set then was modified so that there were several empty rows between segments.

### 3.6 Adding Waypoint Information to the Dataset

After rearranging the dataset into segments, the position fixes for each of the individual segments were tagged according to the source and destination waypoints. This was done using the Google Earth map, as well as reading the test log and the pre-determined waypoint sequence.

The previous waypoint's latitude and longitude were determined using two methods. In the first method, the latitude and longitude coordinates from the field notes were loaded into the spreadsheet. In the second method, the latitude and longitude coordinates of the last ground truth point in the previous segment were used. That is, when walking on the path between A->B->C waypoints, the B->C portion considers the stopping point of the A->B portion as its starting point. This was done to provide two methods of calculating ideal path, since the walking path tended to start/end *near* a waypoint but usually not *on* a waypoint, as in Figure 5.

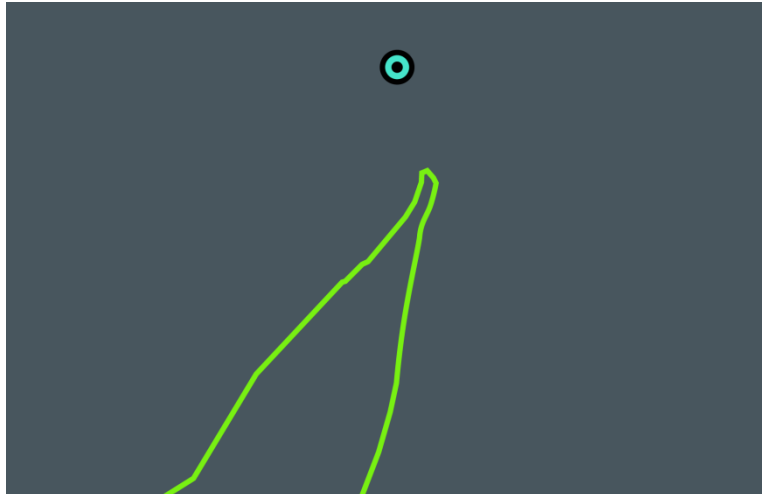


Figure 5.—Mismatch of waypoint and path locations

The destination waypoint's latitude and longitude were taken directly from the field notes, because a similar ambiguity did not exist for the destination.

## 4.0 Data Analysis

### 4.1 Idealized Waypoint to Waypoint Traverse Analysis

The ideal two-dimensional path between two waypoints is a straight line following a single heading. Therefore, the optimal traverse path can be described by a distance and heading calculated between the source and destination waypoints. For this analysis, the WGS84 model for curvature is not followed since the waypoints are close enough together that the error is minimal (<1 m in most cases).

To simplify variable names, a new naming convention is introduced for the following sections. In general, capital letters are used to indicate ground truth position, whereas lowercase letters are used to indicate position recorded by hand (e.g., from field notes) or determined from the filter position fixes. The prefix of the variable name indicates the data type being expressed. Examples are provided:

$h_{pG}$	Heading from previous waypoint ( $p$ ) position based on field notes to current ground truth position ( $G$ )
$h_{pn}$	Heading from previous waypoint ( $p$ ) position based on field notes to next waypoint ( $n$ ) based on field notes
$a_{pGpn}$	Positive angle between the headings of (previous waypoint < $p$ > to current ground truth position) and (previous waypoint < $p$ > to next waypoint < $n$ >)
$d_{PG}$	Distance from previous waypoint ( $P$ ) closest ground truth position to current ground truth position ( $G$ )
$la_p$	Latitude of the previous waypoint ( $p$ ) position based on field notes
$lo_p$	Longitude of the previous waypoint ( $p$ ) position based on field notes
$la_G$	Latitude of the current ground truth position ( $G$ )
$s_f$	Speed of the filter ( $f$ ) determined from filter velocity vectors
$x_f$	X-coordinate for the filter position fix ( $f$ )
$vx_f$	X-coordinate of the filter velocity vector ( $f$ )

The ideal traverse heading function  $h_{pn}$  calculates heading assuming a linear latitude and longitude scale. The longitude is corrected according to the average of the source and destination latitudes. This function is defined in degrees as:

$$h_{pn} := \begin{cases} \tan^{-1} \frac{(lo_n - lo_p) \cos\left(\frac{la_n + la_p}{2}\right)}{(la_n - la_p)} & \text{for } la_n \geq la_p \text{ and } lo_n \geq lo_p \\ 270 + \tan^{-1} \frac{(la_n - la_p)}{(lo_p - lo_n) \cos\left(\frac{la_n + la_p}{2}\right)} & \text{for } la_n \geq la_p \text{ and } lo_n < lo_p \\ 180 + \tan^{-1} \frac{(lo_p - lo_n) \cos\left(\frac{la_n + la_p}{2}\right)}{la_p - la_n} & \text{for } la_n < la_p \text{ and } lo_n < lo_p \\ 90 + \tan^{-1} \frac{(la_p - la_n)}{(lo_n - lo_p) \cos\left(\frac{la_n + la_p}{2}\right)} & \text{for } la_n < la_p \text{ and } lo_n \geq lo_p \end{cases}$$

The ideal traverse heading function operates on small, 90° arcs to avoid ambiguity across platforms and programming languages. There is no correction for crossing the equator or prime meridian, but luckily the test subjects did not walk that far off course! Effectively, this translates into a clockwise angle starting on the positive Y-axis, as shown in Figure 6.

The ideal traverse distance function is defined using the spherical law of cosines (Ref. 1). This equation is computationally simple and provides reasonable accuracy to 1 m. The function is defined:

$$d_{pn} := \left(\frac{40041470}{2\pi}\right) \cos^{-1} [\cos(la_p) \cos(lo_p) \cos(la_n) \cos(lo_n) + \cos(la_p) \sin(lo_p) \cos(la_n) \sin(lo_n) + \sin(la_p) \sin(la_n)]$$

The initial constant quantity represents the radius of the Earth based on the mean circumference. Using trigonometric identities, the equation can be simplified to the more familiar:

$$d_{pn} := \left(\frac{40041470}{2\pi}\right) \cos^{-1} [\cos(la_p) \cos(la_n) \cos(lo_n - lo_p) + \sin(la_p) \sin(la_n)]$$

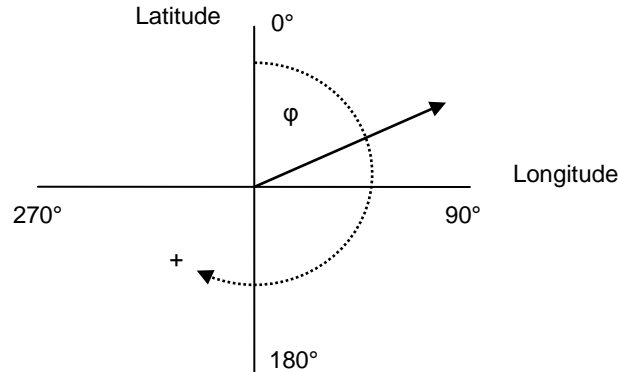


Figure 6.—Mapping of traverse headings

## 4.2 Path Conformance Analysis

One measure of effectiveness of the navigation filter is the ability of the walkback team to adhere to the ideal traverse heading, which would minimize the walking distance. The path conformance can be viewed in terms of the positive  $90^\circ$  distance from the ideal traverse path for each position fix. In other words, path conformance is the distance back to the ideal traverse path, as shown in Figure 7.

Recognizing that the  $90^\circ$  deviation forms a right triangle between the starting location, the current location, and the ideal location, the path conformance can be calculated. The right triangle shown in red (Figure 7) illustrates this concept.

The  $90^\circ$  deviation is calculated from several values. First, a distance is determined between the starting location (i.e., the ground truth location where the previous walk segment ended) and the current ground truth location. The angle between the ideal path and the actual path is also calculated in terms of a reference axis as visualized in Figure 6. Finally, the deviation is calculated using a right-triangle formula. These measurements are illustrated in Figure 8, where  $h_{pG}$  is the heading from the previous waypoint position to the current ground truth position,  $h_{pn}$  is the ideal heading from the previous waypoint to the next waypoint,  $a_{pGpn}$  is the angle between  $h_{pG}$  and  $h_{pn}$ , and  $d_{PG}$  is the distance from the previous waypoint's ground truth position to the current ground truth position.

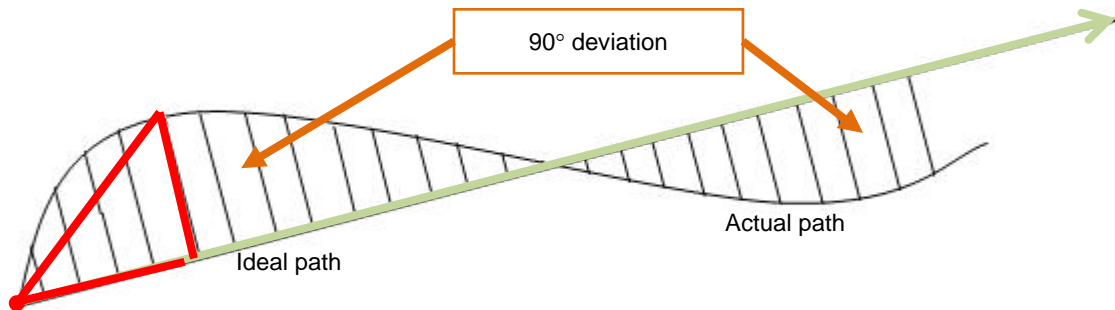


Figure 7.—Path conformance metric

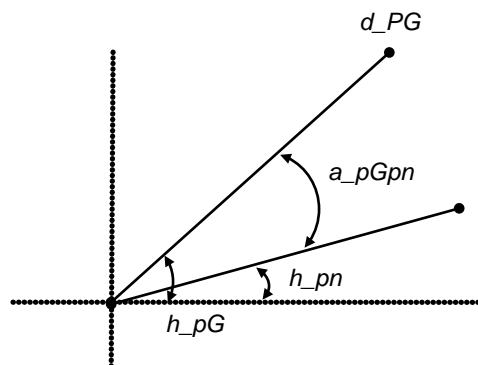


Figure 8.—Visualization of  $90^\circ$  deviation quantities

The formulas for the corresponding 90° deviation quantities in degrees are:

$$h_{pG} := \begin{cases} \tan^{-1} \frac{(lo_G - lo_p) \cos\left(\frac{la_G + la_p}{2}\right)}{(la_G - la_p)} & \text{for } la_G \geq la_p \text{ and } lo_G \geq lo_p \\ 270 + \tan^{-1} \frac{(la_G - la_p)}{(lo_p - lo_G) \cos\left(\frac{la_G + la_p}{2}\right)} & \text{for } la_G \geq la_p \text{ and } lo_G < lo_p \\ 180 + \tan^{-1} \frac{(lo_p - lo_G) \cos\left(\frac{la_G + la_p}{2}\right)}{la_p - la_G} & \text{for } la_G < la_p \text{ and } lo_G < lo_p \\ 90 + \tan^{-1} \frac{(la_p - la_G)}{(lo_G - lo_p) \cos\left(\frac{la_G + la_p}{2}\right)} & \text{for } la_G < la_p \text{ and } lo_G \geq lo_p \end{cases}$$

$$d_{pG} := \cos^{-1} [\cos(la_p) \cos(lo_p) \cos(la_G) \cos(lo_G) + \cos(la_p) \sin(lo_p) \cos(la_G) \sin(lo_G) + \sin(la_p) \sin(la_G)] * 40041470$$

$$a_{pGpn} := \begin{cases} ||h_{pG} - h_{pn}| - 360| & \text{for } (h_{pG} - h_{pn}) > 180 \\ |h_{pG} - h_{pn}| & \text{for } (h_{pG} - h_{pn}) \leq 180 \end{cases}$$

The 90° path deviance is then determined to be:

$$deviance := d_{pG} * \sin(a_{pGpn})$$

This analysis is performed in 2-D primarily to reduce computational complexity. However, it is unlikely that a 3-D measurement would vary greatly. Since the testbed focuses on surface navigation, LECLDS uses a digital elevation map to tie each filter position fix to the Earth's surface. Even if this were not the case, the test subjects still are restricted to ground traverses. The curvature of the earth is insignificant over a typical 1-km test segment.

### 4.3 Walking Path Headings

Several computations can be made to determine how well the test subjects were able to use the navigation system to navigate to a waypoint. Many of these computations, such as walking time or speed, are not compared easily between test subjects of varying physical capabilities. However, in general, all test subjects should be able to use the system to generally walk in the correct direction.

The first equation,  $h_{pG}$ , was calculated for the path conformance analysis. The heading  $h_{pG}$  is determined from previous waypoint position, as determined from field notes, to the current ground truth position. Vectors are drawn for every second of the traverse, and a new heading is computed, as shown in Figure 9.

Since the ground truth position changes during each second of the test,  $h_{pG}$  is recomputed during the entire walk as the heading from the previous waypoint to the new ground truth position. As the distance between the two points becomes larger, the heading tends to smooth out. Eventually,  $h_{pG}$  will converge to the ideal waypoint-to-waypoint heading when the team arrives at the destination waypoint. This concept is applied to a walk segment in Figure 10.

In some cases, it may be better to use  $h_{PG}$ , which is the heading between the final ground truth position of the last segment of the walk and the current ground truth position. This metric is more useful

when the walkback team does not actually approach the waypoint position recorded in the field notes, such as in Figure 10. In general, this only affects the first minute of the walk significantly because the angles tend to converge once the distance is sufficient. Determination of  $h_{PG}$  is shown in Figure 11.

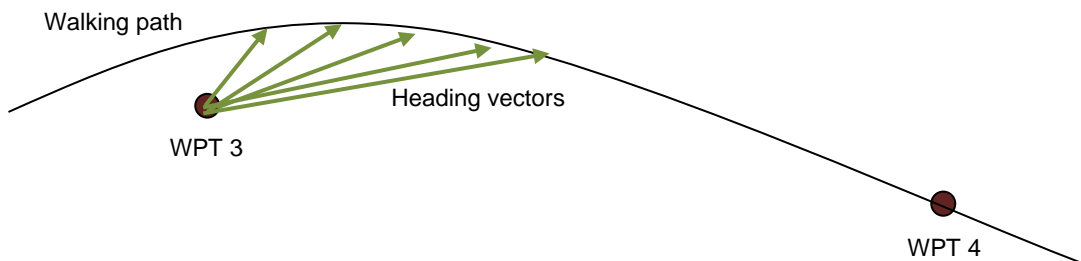


Figure 9.— $h_{pG}$  heading computation

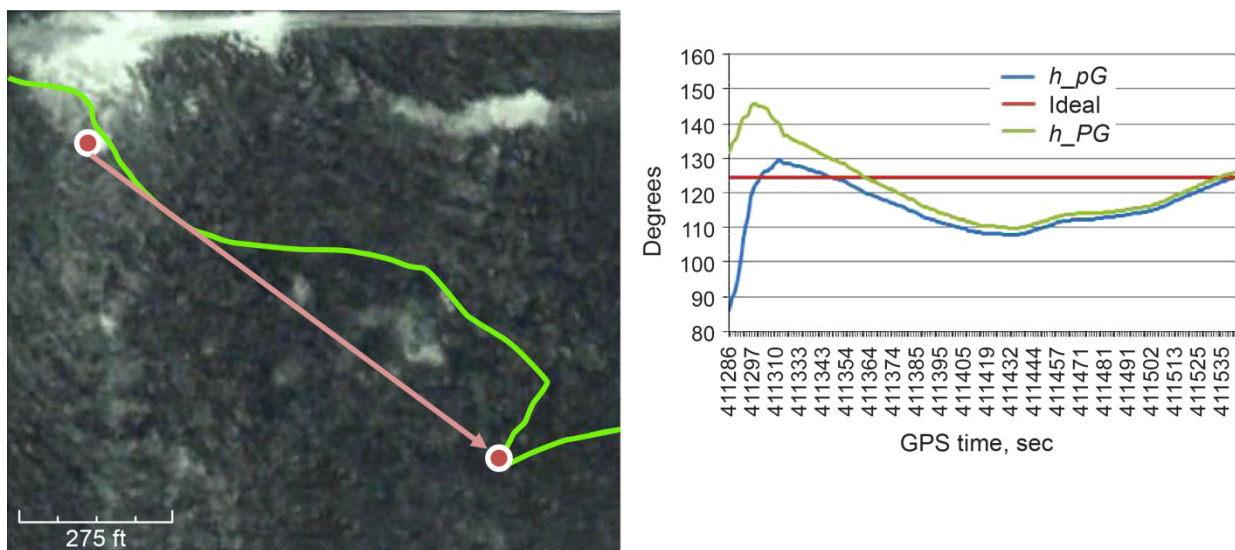


Figure 10.—Example of heading from previous waypoint to current ground truth position

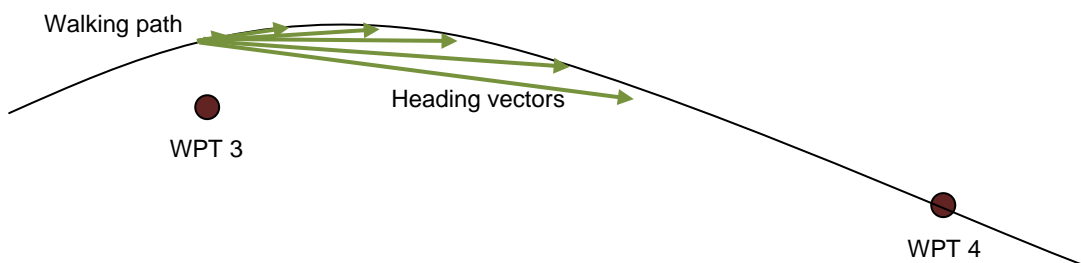


Figure 11.— $h_{PG}$  heading computation

In the ideal case, the walkback team should begin and end each segment of the walk at a waypoint. The waypoint position should match the position in the field notes, which would lead to the two headings  $h_{pG}$  and  $h_{PG}$  being equal. Otherwise, it is difficult to decide which metric to use since they vary subjectively. In the situation where the segment does not begin at a waypoint (e.g., after restarting the system following an error), the system starting coordinates are used for  $la_p$ ,  $lo_p$ ,  $la_P$ , and  $lo_P$ , and therefore  $h_{pG}$  equals  $h_{PG}$ .

The equation for  $h_{PG}$  in degrees is given as:

$$h_{PG} := \begin{cases} \tan^{-1} \frac{(lo_G - lo_P) \cos\left(\frac{la_G + la_P}{2}\right)}{(la_G - la_P)} & \text{for } la_G \geq la_P \text{ and } lo_G \geq lo_P \\ 270 + \tan^{-1} \frac{(la_G - la_P)}{(lo_P - lo_G) \cos\left(\frac{la_G + la_P}{2}\right)} & \text{for } la_G \geq la_P \text{ and } lo_G < lo_P \\ 180 + \tan^{-1} \frac{(lo_P - lo_G) \cos\left(\frac{la_G + la_P}{2}\right)}{la_P - la_G} & \text{for } la_G < la_P \text{ and } lo_G < lo_P \\ 90 + \tan^{-1} \frac{(la_P - la_G)}{(lo_G - lo_P) \cos\left(\frac{la_G + la_P}{2}\right)} & \text{for } la_G < la_P \text{ and } lo_G \geq lo_P \end{cases}$$

Another way of considering heading is to examine  $h_{Gn}$ , which provides the ideal heading from the current ground truth position to the next waypoint (based on field notes). When the test subject walks off of the ideal waypoint-to-waypoint course, it no longer makes sense to use the ideal waypoint-to-waypoint heading as a baseline. The new baseline heading is the one that delivers the shortest path from the current location to the next waypoint, or  $h_{Gn}$ . This is illustrated in Figure 12.

The formula for  $h_{Gn}$  in degrees is given:

$$h_{Gn} := \begin{cases} \tan^{-1} \frac{(lo_n - lo_G) \cos\left(\frac{la_n + la_G}{2}\right)}{(la_n - la_G)} & \text{for } la_n \geq la_G \text{ and } lo_n \geq lo_G \\ 270 + \tan^{-1} \frac{(la_n - la_G)}{(lo_G - lo_n) \cos\left(\frac{la_n + la_G}{2}\right)} & \text{for } la_n \geq la_G \text{ and } lo_n < lo_G \\ 180 + \tan^{-1} \frac{(lo_G - lo_n) \cos\left(\frac{la_n + la_G}{2}\right)}{la_G - la_n} & \text{for } la_n < la_G \text{ and } lo_n < lo_G \\ 90 + \tan^{-1} \frac{(la_G - la_n)}{(lo_n - lo_G) \cos\left(\frac{la_n + la_G}{2}\right)} & \text{for } la_n < la_G \text{ and } lo_n \geq lo_G \end{cases}$$

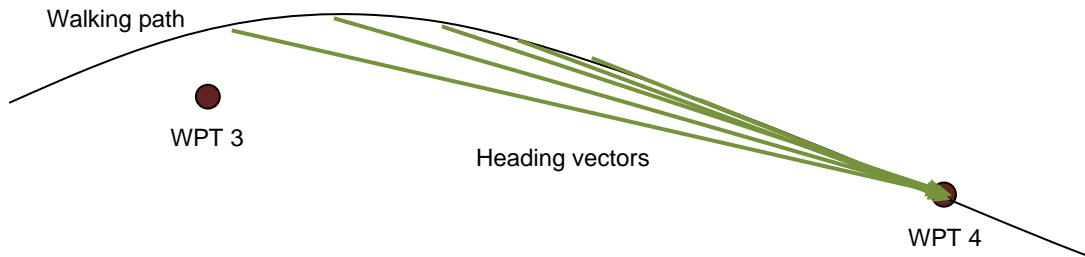


Figure 12.— $h_{Gn}$  heading determination



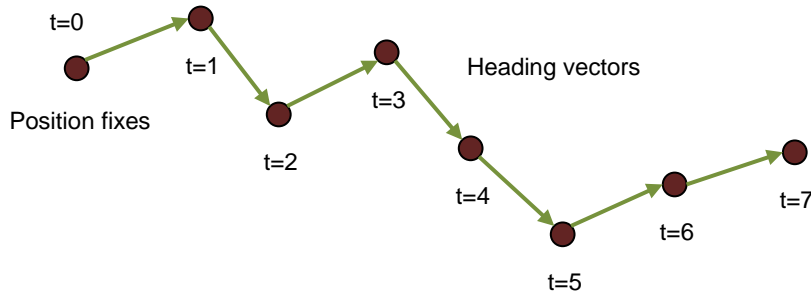


Figure 13.— $h_G$  course computation

The testbed incorporated a digital compass, which provided instantaneous heading. The sampled compass value will be called  $h_D$ . Since the digital compass data is synchronized with the GPS and navigation filter data, the raw headings can be used to compare to the baselines like  $h_{pG}$ ,  $h_{PG}$ , and  $h_{Gn}$ . However, the digital compass can suffer from alignment issues and electromagnetic interference, making a direct comparison difficult between the digital compass heading and position-based courses.

Course, or heading derived from position change, can be used to determine what direction the test subject was walking over a 1-sec interval. This is illustrated in Figure 13. The computation is performed using subsequent ground truth position fixes and the formula for  $h_G$  in degrees:

$$h_G(k) := \begin{cases} \tan^{-1} \frac{(lo_{Gk} - lo_{Gk-1}) \cos(la_{Gk})}{(la_{Gk} - la_{Gk-1})} & \text{for } la_{Gk} \geq la_{Gk-1} \text{ and } lo_{Gk} \geq lo_{Gk-1} \\ 270 + \tan^{-1} \frac{(la_{Gk} - la_{Gk-1})}{(lo_{Gk-1} - lo_{Gk}) \cos(la_{Gk})} & \text{for } la_{Gk} \geq la_{Gk-1} \text{ and } lo_{Gk} < lo_{Gk-1} \\ 180 + \tan^{-1} \frac{(lo_{Gk-1} - lo_{Gk}) \cos(la_{Gk})}{la_{Gk-1} - la_{Gk}} & \text{for } la_{Gk} < la_{Gk-1} \text{ and } lo_{Gk} < lo_{Gk-1} \\ 90 + \tan^{-1} \frac{(la_{Gk-1} - la_{Gk})}{(lo_{Gk} - lo_{Gk-1}) \cos(la_{Gk})} & \text{for } la_{Gk} < la_{Gk-1} \text{ and } lo_{Gk} \geq lo_{Gk-1} \end{cases}$$

Finally, the filter heading displayed to the test subject is also available for analysis. In general, the filter heading is computed the same as  $h_G$ , except with filter position fixes, however the filter can use various smoothing techniques that may affect the display. The filter heading, on a second-by-second basis, is called  $h_f$ .

#### 4.4 Walking Path Heading Errors

Evaluation of the test subject's heading can be done according to several baselines, as mentioned in the previous section. The first technique compares  $h_{pG}$  to  $h_{pn}$  to determine how well the test subject's heading converges to the ideal point-to-point heading. This technique is best used when the test subject begins the walk on a waypoint. The corresponding equation,  $a_{pGpn}$ , was used for the path conformance metric.

When the test does not begin on a waypoint, but close to a waypoint, it is useful to examine heading error between the previous waypoint's ground truth position and the ideal heading. This is often a difficult comparison to make when the distance between the field position and the actual starting position are large; in this case, the shortest vector to the next waypoint is no longer  $h_{pn}$  and other techniques should be used. This equation,  $a_{PGpn}$ , is given as:

$$a_{PGpn} := \begin{cases} \left| |h_{PG} - h_{pn}| - 360 \right| & \text{for } (h_{PG} - h_{pn}) > 180 \\ |h_{PG} - h_{pn}| & \text{for } (h_{PG} - h_{pn}) \leq 180 \end{cases}$$

It is possible to compare the ground truth headings obtained from the digital compass with the ideal traverse heading between waypoints. This comparison should show whether the test subject was pointing in the right direction. In general, the analysis is useful in a qualitative sense, however it might not be as useful for determining filter effectiveness since there can be errors (such as electromagnetic interference from other testbed electronics) that would not cancel when compared to consecutive position fixes. The equation,  $a_{Dpn}$ , is given as:

$$a_{Dpn} := \begin{cases} \left| |h_D - h_{pn}| - 360 \right| & \text{for } (h_D - h_{pn}) > 180 \\ |h_D - h_{pn}| & \text{for } (h_D - h_{pn}) \leq 180 \end{cases}$$

The test subjects were given second-by-second feedback on their current walking heading, as determined using a course computation over subsequent filter position fixes. This heading can be compared versus the ideal heading (which was also displayed on the screen). However, it is important to note that the ideal heading here is the heading between the two waypoints, which is no longer ideal as soon as the test subject walks away from the point-to-point line between the two waypoints. This equation,  $a_{fpn}$ , is given as:

$$a_{fpn} := \begin{cases} \left| |h_f - h_{pn}| - 360 \right| & \text{for } (h_f - h_{pn}) > 180 \\ |h_f - h_{pn}| & \text{for } (h_f - h_{pn}) \leq 180 \end{cases}$$

One of the more useful metrics is to examine error between the filter heading displayed to the test subject and the ideal heading from the current ground truth location to the next waypoint. This is interesting because the baseline (ideal) heading changes on a second-by-second basis as the test subject navigates. The ideal course will always be the straight line between the current location and the next waypoint. This equation,  $a_{fGn}$ , is given as:

$$a_{fGn} := \begin{cases} \left| |h_f - h_{Gn}| - 360 \right| & \text{for } (h_f - h_{Gn}) > 180 \\ |h_f - h_{Gn}| & \text{for } (h_f - h_{Gn}) \leq 180 \end{cases}$$

The accuracy of the filter heading displayed to the user can be compared to the digital compass ground truth heading. Again, this comparison may contain errors that are not cancelled out since the magnetic compass does not have correlated errors with the GPS ground truth. Still, this is a useful metric in observing the general “correctness” of the filter heading being shown to the test subject. Significant errors here would point to the need for a heading sensor (e.g., sun sensor) as opposed to the radiometric course currently used in LECLDS. This equation,  $a_{fD}$ , is given as:

$$a_{fD} := \begin{cases} \left| |h_f - h_D| - 360 \right| & \text{for } (h_f - h_D) > 180 \\ |h_f - h_D| & \text{for } (h_f - h_D) \leq 180 \end{cases}$$

It is also possible to compare the digital compass heading with the ideal heading to the next waypoint. The advantage of this comparison is that it allows analysis to occur on the actual direction the test subject was pointing during the walkback. Other methods that only use position changes indicate the direction the test subject was moving, which does not indicate if the test subject was looking around for the waypoint. This equation,  $a_{DGn}$ , is given as:

$$a_{DGn} := \begin{cases} ||h_{Gn} - h_D| - 360| & \text{for } (h_{Gn} - h_D) > 180 \\ |h_{Gn} - h_D| & \text{for } (h_{Gn} - h_D) \leq 180 \end{cases}$$

The filter heading can be compared with the ground truth course (using consecutive, 1-sec position fixes). This technique is similar to the  $a_{fD}$  calculation, except common errors should be cancelled since both values are determined indirectly from GPS data. The calculation allows the filter heading performance to be examined. This equation,  $a_{fG}$ , is given as:

$$a_{fG} := \begin{cases} ||h_f - h_G| - 360| & \text{for } (h_f - h_G) > 180 \\ |h_f - h_G| & \text{for } (h_f - h_G) \leq 180 \end{cases}$$

The ground truth course also can be compared to the ideal waypoint-to-waypoint heading. This is a useful metric for the beginning of a walk, or as long as  $h_{pn}$  is still a good baseline. The equation for  $a_{Gpn}$  is given as:

$$a_{Gpn} := \begin{cases} ||h_G - h_{pn}| - 360| & \text{for } (h_G - h_{pn}) > 180 \\ |h_G - h_{pn}| & \text{for } (h_G - h_{pn}) \leq 180 \end{cases}$$

#### 4.5 Filter Solution Analysis

One principle behind LECLDS testing is that the accuracy of the data presented to a test subject is a function of the filter being used for the walkback test. This can be characterized in terms of the computation error (versus some ground truth quantity) or derivative characteristics (versus ground truth or some derivative of ground truth). Equations that judge the performance of the filter, independent of the walkback, are considered to be Measurements of Performance (MoPs).

The distance between two filter position estimates,  $d_{f_k f_{k-1}}$ , can be used to show the variance of position fixes around a certain point of time. The sum of all of these values during a test shows the total path length from the perspective of the navigation filter. These values are useful in showing a qualitative comparison of filters, since large variances will result in longer filter paths (versus the ground truth path). However, the individual distance between points is not a useful metric, otherwise, since it is only mathematical error; the test subject will never walk the distance indicated by the filter as long as some filter error exists. The corresponding equations are given as:

$$d_{f(k)f(k-1)} := \sqrt{(x_{f(k)} - x_{f(k-1)})^2 + (y_{f(k)} - y_{f(k-1)})^2 + (z_{f(k)} - z_{f(k-1)})^2}$$

$$d_f := \sum_k d_{f(k)f(k-1)}$$

The positive elevation of the filter also is computed using the Cartesian position fixes. A filter with highly accurate elevation may be more useful for studying geology or other terrain characteristics that are elevation-dependent. In general, the D-RATS data has precise elevation because it uses a digital elevation map as part of the solution computation. The elevation,  $d_{0f}$ , is given as a distance vector from the center of the earth (imaginary center of the Cartesian plane) to the current position fix:

$$d_{0f} := \sqrt{x_f^2 + y_f^2 + z_f^2}$$

Filter speed is determined from output velocity vectors provided by the filtering algorithm. Typically filters will compute the velocity vector using position deltas, however this is not required. The current filter speed from velocity fixes,  $s_f$ , is given as:

$$s_f := \sqrt{vx_f^2 + vy_f^2 + vz_f^2}$$

Filter speed can also be determined directly from the filter position fixes. In fact, since the sampling period is 1 sec for the Desert RATS data set, this quantity ( $s_{f_k f_{k-1}}$ ) is found in the same manner as the position delta,  $d_{f_k f_{k-1}}$ .

$$s_{f(k)f(k-1)} := \sqrt{(x_{f(k)} - x_{f(k-1)})^2 + (y_{f(k)} - y_{f(k-1)})^2 + (z_{f(k)} - z_{f(k-1)})^2}$$

The filter heading, determined from 1-sec position fixes, is also a derivative quantity based on position fixes. The filter heading,  $h_{f_k}$ , can be combined with the filter speed  $s_{f_k f_{k-1}}$  to provide an interesting look at the vector of the consecutive position fixes. In general, this vector should follow the test subject when the test subject's location change exceeds the filter error. When the test subject stands still, the vector is less useful because the filter creates a scatter of position fixes around the true location; the vector simply maps the error. The corresponding equation for filter heading is given in degrees as:

$$h_f(k) := \begin{cases} \tan^{-1} \frac{(lo_{f_k} - lo_{f_{k-1}}) \cos(la_{f_k})}{(la_{f_k} - la_{f_{k-1}})} & \text{for } la_{f_k} \geq la_{f_{k-1}} \text{ and } lo_{f_k} \geq lo_{f_{k-1}} \\ 270 + \tan^{-1} \frac{(la_{f_k} - la_{f_{k-1}})}{(lo_{f_{k-1}} - lo_{f_k}) \cos(la_{f_k})} & \text{for } la_{f_k} \geq la_{f_{k-1}} \text{ and } lo_{f_k} < lo_{f_{k-1}} \\ 180 + \tan^{-1} \frac{(lo_{f_{k-1}} - lo_{f_k}) \cos(la_{f_k})}{la_{f_{k-1}} - la_{f_k}} & \text{for } la_{f_k} < la_{f_{k-1}} \text{ and } lo_{f_k} < lo_{f_{k-1}} \\ 90 + \tan^{-1} \frac{(la_{f_{k-1}} - la_{f_k})}{(lo_{f_k} - lo_{f_{k-1}}) \cos(la_{f_k})} & \text{for } la_{f_k} < la_{f_{k-1}} \text{ and } lo_{f_k} \geq lo_{f_{k-1}} \end{cases}$$

#### 4.6 Ground Truth Solution Analysis

Many of the same metrics can be applied to the ground truth measurements; however, the interpretation of these values is slightly different. For example, the position delta is a more useful metric since it is a better representation of the actual distance walked on a second-to-second basis. The ground truth data will contain some error, but the error is considered to be much less than that of the filter.

The distance between two ground-truth position fixes ( $d_{G_k G_{k-1}}$ ), the sum of those distances, and the elevation ( $d_{0G}$ ) are calculated similar to the equations above:

$$d_{G(k)G(k-1)} := \sqrt{(x_{G(k)} - x_{G(k-1)})^2 + (y_{G(k)} - y_{G(k-1)})^2 + (z_{G(k)} - z_{G(k-1)})^2}$$

$$d_{0G} := \sqrt{x_G^2 + y_G^2 + z_G^2}$$

The ground truth speed ( $s_G$ ) is calculated in a slightly different manner. The Novatel GPS receiver provides velocity along the X, Y, and Z Cartesian axes using instantaneous Doppler measurements, with a small latency of approximately 0.15 sec. Therefore, the speed computed using the receiver measurements

will not correspond identically to the filter speed, which is computed using position deltas. The ground truth speed and digital compass data are both distinct from other testbed measurements, since they are instantaneous. The quantity  $s_G$  is calculated according to the equation:

$$s_G := \sqrt{vx_G^2 + vy_G^2 + vz_G^2}$$

## 4.7 Filter Error Analysis

The overall performance of the navigation filter can be characterized in terms of its position accuracy. All of the other filter quantities discussed above are derived from the filter position, therefore it follows that a highly accurate filter position will lead to a highly accurate speed, heading, etc. The solution position error ( $e_{pos}$ ) is computed directly from the filter position and ground truth position:

$$e_{pos} := \sqrt{(x_f - x_G)^2 + (y_f - y_G)^2 + (z_f - z_G)^2}$$

The positive elevation error ( $e_{elev}$ ) of the filter position estimate is computed using the imaginary vector quantities discussed above, originating at the center of the Cartesian axis.

$$e_{elev} := |d_{0f} - d_{0G}|$$

The positive speed error ( $e_{speed}$ ) of the filter speed estimate is determined from the filter velocity estimates and the ground truth speed. It is important to keep in mind that the ground truth speed is determined using instantaneous Doppler measurements with slight delay. Ideally, the filter also should deliver instantaneous speed updates to the user.

$$e_{speed} := |s_f - s_G|$$

The position delta speed error ( $e_{speed\_posdelta}$ ) compares the filter speed estimate determined using the position deltas between subsequent fixes and the instantaneous ground truth speed. When the test subject is walking at a relatively constant rate, these quantities should be very close. It is also possible to compare the filter position delta with the ground truth position delta, however that is not done here because the instantaneous Doppler velocities would be more accurate at the time when the speed value is updated.

$$e_{speed\_posdelta} := |s_{f(k)f(k-1)} - s_G|$$

## 4.8 Velocity Made Good

One useful Measure of Effectiveness (MoE) is the velocity made good ( $VMG$ ).  $VMG$  is the effective velocity of the test subject along the ideal path from the current ground truth location to the next waypoint. If the test subject is on the proper course, the magnitude of the  $VMG$  will be equal to the magnitude of the test subject's velocity. If not, the  $VMG$  will always be smaller than the velocity. Effectiveness can be determined as the ratio of  $VMG$  to velocity.

The equation for  $VMG$  is given as:

$$VMG := \frac{(x_n - x_G) * vx_G + (y_n - y_G) * vy_G + (z_n - z_G) * vz_G}{\sqrt{(x_n - x_G)^2 + (y_n - y_G)^2 + (z_n - z_G)^2}}$$

## 5.0 Summary of Data Analysis Metrics

Table II contains a summary of the metrics discussed in this paper with some commentary on application.

TABLE II.—DATA ANALYSIS METRICS AND DISCUSSION

Metric	Description/commentary
$h_{pn}$	Ideal traverse heading function; provides the ideal heading from one waypoint to the next. <ul style="list-style-type: none"> <li>Used to determine the most efficient 2-D heading between waypoints.</li> </ul>
$d_{pn}$	Ideal traverse distance function; provides the ideal distance from one waypoint to the next. <ul style="list-style-type: none"> <li>Used to determine the most efficient 2-D route between waypoints.</li> </ul>
$h_{pG}$	Heading from the previous waypoint location to the current ground truth (GT) position. <ul style="list-style-type: none"> <li>Used as part of the 90° path deviance calculation; assumes the test subject started at the waypoint. This metric will conform to the ideal heading (<math>h_{pn}</math>) as the test subject approaches the next waypoint.</li> </ul>
$d_{PG}$	Distance from the GT position closest to the previous waypoint to the current GT position. <ul style="list-style-type: none"> <li>Provides the distance baseline for the 90° path deviance calculation.</li> </ul>
$deviance$	90° path deviation. <ul style="list-style-type: none"> <li>A very useful metric for examining path conformance. However, the metric assumes that the navigation system is guiding the test subject back to the ideal path between waypoints.</li> </ul>
$h_{PG}$	Heading between the final GT position of the previous segment and the current GT position. <ul style="list-style-type: none"> <li>More useful than <math>h_{pG}</math> when the test subject does not begin the segment at the exact waypoint location.</li> </ul>
$h_{Gn}$	Heading from the current GT location to the next waypoint. <ul style="list-style-type: none"> <li>Useful when the navigation system does not guide the test subject back to the ideal path. This heading represents the shortest line between the current location and the destination waypoint.</li> </ul>
$h_D$	Heading determined from the GT digital compass. <ul style="list-style-type: none"> <li>Only used for ground analysis. Often this metric is not valid as a comparison since it records the direction the test subject is pointed and not necessary the direction of motion.</li> </ul>
$h_G$	Heading determined using the change in GT position over a 1-sec interval. <ul style="list-style-type: none"> <li>Best comparison to <math>h_f</math>, when <math>h_f</math> is derived directly from position, since it uses the same computation method.</li> </ul>
$h_f$	Heading determined using the change in filter position over a 1-sec interval. <ul style="list-style-type: none"> <li>This is the value shown to the test subject, possibly with some smoothing or averaging depending on the filter.</li> </ul>
$a_{pGpn}$	Angle between the headings from previous waypoint to current GT position and ideal waypoint-to-waypoint. <ul style="list-style-type: none"> <li>The 'pG' quantity is useful for seeing how well test subjects were able to navigate away from the starting waypoint.</li> <li>However, 'pn' only applies as long as the test subject stays on the ideal traverse path.</li> </ul>
$a_{PGpn}$	Angle between the headings from previous waypoint GT location to current GT position and ideal waypoint-to-waypoint. <ul style="list-style-type: none"> <li>'PG' works well when the test subject does not start on top of the waypoint.</li> <li>However, 'pn' is not a good comparison since the test subject does not start at point 'p'.</li> </ul>
$a_{Dpn}$	Angle between digital compass heading and the ideal waypoint-to-waypoint heading. <ul style="list-style-type: none"> <li>'D' is a true heading indicator, unlike all of the GPS-based course indicators.</li> <li>'D' indicates which direction the test subject is pointing, not which direction they are moving.</li> <li>'pn' baseline only applies as long as the test subject stays on the ideal line.</li> <li>'D' tends to have magnetic/electric errors that can confuse analysis of the data.</li> </ul>
$a_{fpn}$	Angle between the heading shown to the test subject on the display and the ideal waypoint-to-waypoint heading. <ul style="list-style-type: none"> <li>'f' is the heading seen by the test subject on the display, so it is well-known to the test subject.</li> <li>'pn' baseline only applies as long as the test subject stays on the ideal line.</li> </ul>
$a_{fGn}$	Angle between the displayed heading and the ideal heading from current GT location to the next waypoint. <ul style="list-style-type: none"> <li>'f' is the heading seen by the test subject on the display, so it is well-known to the test subject.</li> <li>'Gn' baseline is fluid and will re-compute the ideal heading based on the current position.</li> <li>However, 'Gn' baseline is not known by the test subject, since the ground truth location is not known.</li> </ul>

TABLE II.—DATA ANALYSIS METRICS AND DISCUSSION

Metric	Description/commentary
$a_{fD}$	Angle between the filter heading and the digital compass heading. <ul style="list-style-type: none"> <li>Provides useful analysis of deviation between filter course and instantaneous heading.</li> <li>However, '<math>f</math>' and '<math>D</math>' come from different sensors and might not be 1-to-1 comparable in all situations.</li> </ul>
$a_{DGn}$	Angle between the digital compass heading and the ideal heading to the next waypoint from current GT location. <ul style="list-style-type: none"> <li>Metric could be used to observe if the test subject is looking around (turning) for the waypoint.</li> <li>It is generally not that useful to compare pointing direction with walking direction.</li> </ul>
$a_{fG}$	Angle between the filter heading and the ground truth heading using 1-sec position deltas. <ul style="list-style-type: none"> <li>'<math>f</math>' could have smoothing that would be useful to compare to a metric without processing like '<math>G</math>'.</li> <li>'<math>G</math>' tends to have high levels of error when ground speed is low.</li> </ul>
$a_{Gpn}$	Angle between the ground truth 1-sec heading and the ideal waypoint-to-waypoint heading. <ul style="list-style-type: none"> <li>Similar to <math>a_{fpn}</math>, provides insight into actual walking direction versus ideal heading.</li> <li>'<math>pn</math>' baseline only applies as long as the test subject stays on the ideal line.</li> </ul>
$d_{f(k)f(k-1)}$	Distance between consecutive filter position fixes. <ul style="list-style-type: none"> <li>Useful only as a qualitative indicator of filter position stability.</li> </ul>
$d_{0f}$	Distance from the center of the Cartesian plane to the current filter position. <ul style="list-style-type: none"> <li>When compared to an elevation map, provides insight into the filter's ability to tie solutions to the surface.</li> <li>Should remain relatively constant, plus or minus small terrain variations, for surface navigation.</li> </ul>
$s_f$	Speed determined by the filter. <ul style="list-style-type: none"> <li>Typically equivalent to <math>d_{f(k)f(k-1)}</math> unless the speed algorithm is separate from the position algorithm.</li> </ul>
$d_{G(k)G(k-1)}$	Distance between consecutive GT position fixes. <ul style="list-style-type: none"> <li>Quite useful when summed for a given segment or test; provides a good estimate of total distance travelled.</li> </ul>
$d_{0G}$	Distance from the center of the Cartesian plane to the current GT position. <ul style="list-style-type: none"> <li>Indicates the GPS' view of the current elevation in WGS84; comparable to <math>d_{0f}</math>.</li> </ul>
$s_G$	Speed determined by the GPS unit. <ul style="list-style-type: none"> <li>Typically an instantaneous speed, only comparable to <math>s_f</math> when walking speed is constant across the navigation filter update rate (1 sec here).</li> </ul>
$e_{pos}$	Error, RSS, of the filter position versus the GT position. <ul style="list-style-type: none"> <li>Standard metric to indicate filter performance for a given position fix.</li> </ul>
$e_{elev}$	Error, absolute value, of the filter elevation versus the GT elevation. <ul style="list-style-type: none"> <li>Indicates the filter's ability to clamp the solution to the surface.</li> <li>Also can indicate coordinate system mismatches between the GPS and navigation filter.</li> </ul>
$e_{speed}$	Error, absolute value, of the filter speed estimate versus instantaneous GPS speed. <ul style="list-style-type: none"> <li>Not very useful unless the filter can also provide near-instantaneous speed estimates.</li> <li>Typically this will provide better insight into filter position stability than speed.</li> <li>Depending on implementation, similar to <math>e_{speed\_posdelta}</math>, which uses position fix deltas to generate speed.</li> </ul>
$VMG$	Velocity made good, effective velocity of the test subject from the current GT position to the next waypoint. <ul style="list-style-type: none"> <li>Interesting method of analyzing the test subject's progress in reaching a waypoint independent of heading.</li> <li>Can be zero for perpendicular travel or negative for travel in the wrong direction.</li> </ul>

## 6.0 Recommendations

The data analysis process provided a great deal of insight into the considerations needed for designing a useful test procedure. Data analysis touches every aspect of the data, from time alignment methods, to data formats, to the underlying research objectives and test methodology.

The time alignment procedure for D-RATS 2009 was sufficient to reconstruct the dataset, however this needed to be done by hand and took a great deal of time. There were four primary timestamps used by LECLDS: a system timestamp (ns), the GPS time (ms), processor ticks (ticks/sec), and the handwritten test log timestamp (min). It was difficult to tie the handwritten test log timestamp to the other timestamps

since the lack of resolution and unknown bias was significant. It would be better if all of the logs shared a common timestamp with similar resolution; for example, record the test log using a GPS timestamp with accuracy to the nearest second.

LECLDS used multiple log files for the different testbed sensor data. This was most convenient at the time, and allowed development of the software to occur independently. However, a single, integrated log file would have been easier to analyze. It would have also solved many of the time alignment issues.

The waypoint locations often did not correspond with the walking path. It is possible that this was due to the use of a separate, handheld GPS receiver to compute the waypoint location. Future tests should use the LECLDS GPS receiver to compute the waypoint position for consistency. It complicated analysis when the test subject did not end at the position of the destination waypoint.

The display software was written to take the test subject to the next waypoint using the most direct route. This makes sense from a logistics sense, however in a real lunar scenario it is possible that there would be a safety risk in using this approach. Future tests should consider taking the test subject back to the original traverse path between waypoints, as that might be the safest path to use to traverse the area. This would simplify analysis and make path conformance a stronger metric.

A bit of hand-waving was done when removing a collection of position fixes recorded around the starting or ending waypoints. It would have made the analysis more accurate if the test subject had some method of indicating the time of arrival (to the nearest second) and departure at a waypoint. It might be interesting to conduct the test without physical waypoints; that is, there would be no “cones” or visual clues in the field to indicate arrival at a waypoint. The test subject would have to rely on the display to accomplish the test objectives.

Walking speed was not controlled in the test, since different test subjects would walk at different speeds depending on the terrain. If the test subjects were instructed to walk as quickly as possible (e.g., targeting 10 km in 2 hr), then the walking speed might be a good indicator of the test subject’s level of comfort with the system accuracy.

## **7.0 Conclusions**

The data analysis techniques presented in this paper represent only a small subset of all of the possible methods of analyzing the data. These techniques provided insight into redesigns of the LECLDS testbed and changes in the test procedures, with the intention of collecting more useful data in the future.

The Lunar Surface Navigation team at GRC conducted additional testing at the Desert RATS 2010 event in September 2010. The test incorporated many of the recommended improvements, including uniform time alignment, strictly-defined waypoint locations, navigation back to a predefined ideal path, and removal of cones from the test site. As of this report, revised data analysis metrics and methodology have not yet been defined.

## **Reference**

1. “Calculate distance and bearing between two Latitude/Longitude points using Haversine formula,” Movable Type Scripts. Available at: <http://www.movable-type.co.uk/scripts/latlong.html>.



REPORT DOCUMENTATION PAGE				Form Approved OMB No. 0704-0188	
<p>The public reporting burden for this collection of information is estimated to average 1 hour per response, including the time for reviewing instructions, searching existing data sources, gathering and maintaining the data needed, and completing and reviewing the collection of information. Send comments regarding this burden estimate or any other aspect of this collection of information, including suggestions for reducing this burden, to Department of Defense, Washington Headquarters Services, Directorate for Information Operations and Reports (0704-0188), 1215 Jefferson Davis Highway, Suite 1204, Arlington, VA 22202-4302. Respondents should be aware that notwithstanding any other provision of law, no person shall be subject to any penalty for failing to comply with a collection of information if it does not display a currently valid OMB control number.</p> <p>PLEASE DO NOT RETURN YOUR FORM TO THE ABOVE ADDRESS.</p>					
1. REPORT DATE (DD-MM-YYYY) 01-11-2011		2. REPORT TYPE Technical Memorandum		3. DATES COVERED (From - To)	
4. TITLE AND SUBTITLE Data Analysis Techniques for a Lunar Surface Navigation System Testbed				5a. CONTRACT NUMBER	
				5b. GRANT NUMBER	
				5c. PROGRAM ELEMENT NUMBER	
6. AUTHOR(S) Chelmins, David; Sands, O., Scott; Swank, Aaron				5d. PROJECT NUMBER	
				5e. TASK NUMBER	
				5f. WORK UNIT NUMBER WBS 903184.04.20.03.02.01	
7. PERFORMING ORGANIZATION NAME(S) AND ADDRESS(ES) National Aeronautics and Space Administration John H. Glenn Research Center at Lewis Field Cleveland, Ohio 44135-3191				8. PERFORMING ORGANIZATION REPORT NUMBER E-17789	
9. SPONSORING/MONITORING AGENCY NAME(S) AND ADDRESS(ES) National Aeronautics and Space Administration Washington, DC 20546-0001				10. SPONSORING/MONITOR'S ACRONYM(S) NASA	
				11. SPONSORING/MONITORING REPORT NUMBER NASA/TM-2011-217113	
12. DISTRIBUTION/AVAILABILITY STATEMENT Unclassified-Unlimited Subject Category: 32 Available electronically at <a href="http://www.sti.nasa.gov">http://www.sti.nasa.gov</a> This publication is available from the NASA Center for AeroSpace Information, 443-757-5802					
13. SUPPLEMENTARY NOTES					
14. ABSTRACT NASA is interested in finding new methods of surface navigation to allow astronauts to navigate on the lunar surface. In support of the Vision for Space Exploration, the NASA Glenn Research Center developed the Lunar Extra-Vehicular Activity Crewmember Location Determination System and performed testing at the Desert Research and Technology Studies event in 2009. A significant amount of sensor data was recorded during nine tests performed with six test subjects. This paper provides the procedure, formulas, and techniques for data analysis, as well as commentary on applications.					
15. SUBJECT TERMS Surface navigation; Lunar surface; Radio navigation; Positioning					
16. SECURITY CLASSIFICATION OF:			17. LIMITATION OF ABSTRACT	18. NUMBER OF PAGES 27	19a. NAME OF RESPONSIBLE PERSON
a. REPORT U	b. ABSTRACT U	c. THIS PAGE U			STI Help Desk (email:help@sti.nasa.gov)
					19b. TELEPHONE NUMBER (include area code) 443-757-5802



